RESEARCH PAPER

PCCP
www.rsc.org/pccp

The oxidation of trivalent chromium at polycrystalline gold electrodes

Christine M. Welch, Michael E. Hyde, Olga Nekrassova and Richard G. Compton*

Physical and Theoretical Chemistry Laboratory, University of Oxford, South Parks Road, Oxford, UK, OX1 3QZ . E-mail: richard.compton@chem.ox.ac.uk; Fax: +44 1865 275410; Tel: +44 1865 275413

Received 19th March 2004, Accepted 21st April 2004
First published as an Advance Article on the web 14th May 2004

The electrochemical oxidation of Cr(III) to Cr(VI) species was examined in aqueous solution. The responses of boron doped diamond, glassy carbon and gold electrodes were probed towards the oxidation of trivalent chromium over a wide pH range (1.0–13.0). High quality voltammetric profiles were found to appear only at a gold electrode and in solutions of pH greater than 12. It was found that the oxidation reaction proceeds via a multi-step mechanism, where the first electron transfer is electrochemically irreversible and rate-determining, followed by two fast electron transfers. DIGISIM was successfully utilized to model the experimentally obtained data. The oxidation was additionally found to involve OH^- ions, at potentials where these are adsorbed at the gold electrode surface. AFM measurements were carried out to complement these findings.

1. Introduction

The electrochemistry and the speciation of chromium compounds is a very important task due to the contrasting impact of the two environmentally relevant valence states of chromium, Cr(III) and Cr(VI). Hexavalent chromium is reported to be toxic[1,2] due to its high oxidation potential and ability to cross cellular membranes via non-specific anion carriers,[3] whereas trivalent chromium is considered to be relatively harmless, although it was shown that Cr(III) is more effective than Cr(VI) in causing genotoxicity in cell-free systems.[4,5] The main sources of anthropogenic chromium pollution in ground water are plating industries, cooling towers, timber treatment,[6] leather tanning, wood preservation and steel manufacturing.[7]

Numerous studies have been reported on the Cr(II)/Cr(III) couple at mercury electrodes [see *e.g.* ref. 8 and refs. within], although we found no report on Cr(III) oxidation at mercury electrodes in the literature as would be expected from the relative ease of oxidation of mercury compared with Cr(III). Turning to solid electrodes, direct oxidation of trivalent chromium has been studied at smooth and platinised platinum microelectrodes[9] and metal oxide electrodes.[10] Recently an analytical procedure for the detection of Cr(III) in pharmaceutical compounds at pH 8 has been claimed on natural and synthetic diamond paste electrodes.[11] However, no report has been published on the oxidation of Cr(III) at gold electrodes; this is the primary subject of the work reported below.

In this paper the electrochemical oxidation of trivalent chromium is studied at various macroelectrode substrates (boron doped diamond, glassy carbon and gold) over a wide pH range (1.0–13.0); for pH $>$ 13 we note that Cr(III) is reported to be electroactive on platinum.[9] Of the three materials studied in our work, it was found that only a gold electrode allowed us to obtain a distinctive voltammetric profile towards the oxidation of trivalent chromium at the concentrations studied and then only in very alkaline conditions (pH >12). Different electrode pre-treatments of the gold electrode are examined and it is suggested that trivalent chromium oxidation process occurs via reaction with OH^- species, which are adsorbed at the gold electrode. This study is complemented by AFM studies.

2. Experimental

Electrochemical measurements were performed with an Autolab PGSTAT 30 potentiostat (Eco-Chimie, Netherlands). Glassy carbon (GC) (0.07 cm^2, BAS Technocol, UK), boron doped diamond (BDD) (0.25 cm^2, Element Six Ltd, UK) or gold (0.07 cm^2, made in house) electrodes served as working electrodes. A platinum wire provided the counter electrode with a saturated calomel reference electrode (SCE, Radiometer, Denmark) completing the cell assembly. The GC electrode was polished between each series of experiments with 1 μm particle size diamond pastes (Kemet, UK). The gold working electrode was polished between each series of experiments with alumina micropolish II (Buehler, UK) of decreasing particle size (2 to 0.3 μM). Unless stated otherwise (section 3.5), the gold electrode surface was activated prior to each series of additions/changing scan rates *via* cycling ten times (50 mV s^{-1}) from −0.5 V to +0.6 V (*vs.* SCE) in solution of 0.1 M KOH, de-oxygenated with N_2 stream, with the last scan stopped at −0.5 V. The BDD electrode had undergone no surface pre-treatment. All experiments were carried out in a cell of volume 20 cm^3 and at a temperature of 20 ± 2 °C.

The microscope used was a Digital Instruments (Santa Barbara, USA) Multimode SPM, operating in TappingMode with a "J" scanner, having a lateral range of 125 × 125 μm and a vertical range of 5 μm.

The AFM measurements were performed in a Digital Instruments TappingMode fluid cell (having an approximate volume of 0.5 cm^3), using a standard three electrode configuration described above. Once in position on the AFM scanner head, the solution was fed into one of the inlets of the cell using a syringe until it was full and no bubbles remained. One of the other inlets had a platinum counter electrode placed in it, and the third was used as a fluid outlet. The outlet tube was clipped shut, and the partly filled input syringe used as a reservoir, into which the saturated calomel reference electrode (Radiometer) was placed.

$Cr(NO_3)_3$ and $Cr_2(SO_4)_3$ and other reagents were obtained from Aldrich; these were of the highest grade available ($>$99%) and used without further purification. All solutions and subsequent dilutions were prepared using deionised water

DOI: 10.1039/b404243c

from Vivendi (Vivendi, UK) UHQ grade water system with a resistivity of not less than 18 MΩ cm.

3. Results and discussions

3.1 Speciation of the chromium species

The examination of the Pourbaix diagram[12] for chromium shows that in solutions above pH 7, chromium(VI) is present only in the form of CrO_4^{2-}. Chromium(III) occurs as $Cr(OH)_3$ in solutions of pH between 7 and 12 and in the form of CrO_2^- in solutions above pH 12.

The overall electrochemical oxidation of Cr(III) for pH >12 proceeds *via* the reaction outlined below: $CrO_4^{2-} + 3e^- + 4H^+ \rightleftharpoons CrO_2^- + H_2O$ The standard electrode potential is given by eqn. (1):

$$E^0 = 0.945 - 0.0788\ \text{pH}[12] \qquad (1)$$

3.2 Initial studies of the reaction

The initial electrochemical oxidation of 500 μM trivalent chromium was investigated at various electrode materials (BDD, GC, Au) in pH 1.0 (0.1 M HCl), pH 4.0 (0.1 M citrate buffer, 0.1 M KCl), pH 8.0 (0.1 M phosphate buffer) and pH 13 (0.1 M KOH) solutions. In contrast to chromium (VI), which was found to be electroactive at several electrode substrates,[13] trivalent chromium at the concentrations studied was observed to be electrochemically active only at the gold electrode and only in very alkaline conditions (with pH greater than 12). This might be tentatively explained by the "enhanced activity" of gold electrodes in alkaline conditions, attributed possibly to the formation of some kind of oxygen containing species, either OH^-[14] or hydrous gold oxide,[15] which is more favorable in alkaline media. We consider these ideas further later in this paper.

Fig. 1 illustrates the response of an activated (see Experimental section) gold electrode in 0.1 M KOH (dashed line). This reveals an oxidation process at +0.40 V (*vs.* SCE), which can be attributed to a formation of anodic "oxide" film[16] on the electrode surface, with a subsequent reduction process at +0.07 V (*vs.* SCE). It should be noted that the similar behaviour was observed at both electrochemically roughened and mechanically polished gold.[16] A new oxidation wave emerged at +0.07 V upon addition of 100 μM trivalent chromium nitrate to 0.1 M KOH and continued to grow with further additions of chromium (III) nitrate and could be attributed to the oxidation of the trivalent chromium species to the hexavalent chromium species. This process was found to be chemically irreversible in the potential range studied. The reduction wave observed during the reverse scan at +0.07 V was found to be independent of the concentration of Cr(III) present and can be rationalised as a reduction of the generated oxide film[16,17] as it is also observed in blank 0.1 M KOH. The increase in oxidation peak current measured at +0.07 V was found to be linear with concentration of trivalent chromium added to 0.1 M KOH in the range of 100 to 1000 μM (gradient = 3.2×10^{-2} A M^{-1}, $R^2 = 0.98$). In order to attribute the oxidation process at +0.07 V to the oxidation of chromium species, similar experiments were carried out using trivalent chromium sulphate. The voltammograms obtained (not shown) revealed analogous oxidation behaviour at +0.07 V, indicating that the process is not influenced by the anions present at least in the concentration ranges studied.

Tafel analysis of voltammograms corresponding to the oxidation of 500 μM Cr(III) (scan rate = 50 mV s^{-1}) plotted as potential *vs.* log(current) produced a value of 95 mV per decade, which suggests the possibility of a multi-step electron transfer. Using eqn. (2):

$$b = \frac{2.303RT}{\alpha_{an} n' F} \qquad (2)$$

where b (in V) is the slope of potential against log(current), α_{an} is the electron transfer coefficient for the anodic process and n' is the number of electrons transferred in the rate-determining step (RDS), a value of 0.62 for $\alpha_{an}n'$ was determined. This suggests that it is the transfer of the first electron to Cr(III) which is electrochemically irreversible, so that $n' = 1$ and $\alpha_{an} = 0.62$.

The increase in the oxidation current at +0.4 V (*vs.* SCE) observed with increasing additions of Cr(III) reflects the "tail" of the trivalent chromium oxidation wave and is not related to the formation of the additional gold oxide film. The latter remains constant as can be seen from the magnitude of the reduction peak current.

In order to obtain further insights the response of 500 μM trivalent chromium was examined at various scan rates in 0.1 M KOH. The voltammograms obtained at the activated gold electrode are shown in Fig. 2. It can be seen that the oxidation peak potential shifts with increasing scan rates towards a more positive potential, confirming the irreversibility of the electrochemical reaction. The corresponding plot of peak current against square root of scan rate (10–400 mV s^{-1}) was found to be linear, suggesting that the process is diffusion rather than surface controlled.

An approximate diffusion coefficient value was calculated based on experimental data and the eqn. (3) for diffusion controlled electrochemically irreversible reaction in which the first electron transfer is rate-determining:

$$I_{peak} = (2.99 \times 10^5) n(\alpha_{an} n')^{1/2} A C_0 D^{1/2} V^{1/2} \qquad (3)$$

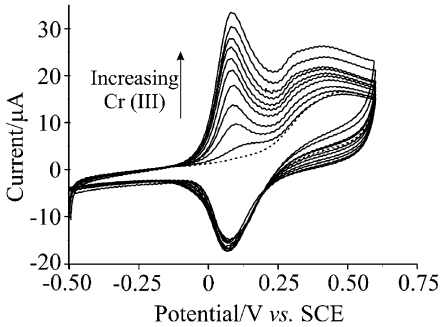

Fig. 1 Cyclic voltammograms (scan rate = 50 mV s^{-1}) detailing the response of increasing additions of aqueous Cr(III) (100–1000 μM) in 0.1 M KOH at an electrochemically activated (10 cycles from −0.5 V to +0.6 V in 0.1 M KOH) gold electrode. Dashed line: response of the activated gold electrode recorded in 0.1 M KOH (scan rate = 50 mV s^{-1}).

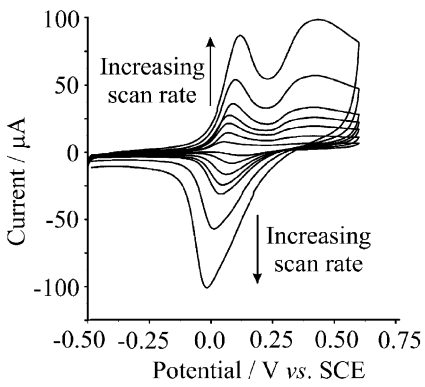

Fig. 2 Cyclic voltammograms detailing the response of 500 μM Cr (III) towards increasing scan rates (10–400 mV s^{-1}) at an activated (10 cycles from −0.5 V to +0.6 V in 0.1 M KOH) gold electrode in 0.1 M KOH.

$$\overset{III}{Cr}O_2^- + OH^- \xrightarrow{E_1^0} e^- + H^+ + \overset{IV}{Cr}O_3^{2-} \qquad \text{RDS}$$

$$\overset{IV}{Cr}O_3^{2-} \xrightarrow{E_2^0} e^- + \overset{V}{Cr}O_3^- \qquad \text{Fast}$$

$$\overset{V}{Cr}O_3^- + OH^- \xrightarrow{E_3^0} e^- + H^+ + \overset{VI}{Cr}O_4^{2-} \qquad \text{Fast}$$

$$Total: CrO_2^- + 2OH^- \rightarrow 3e^- + 2H^+ + CrO_4^{2-} \text{ or } CrO_2^- + 2H_2O \rightarrow 3e^- + 4H^+ + CrO_4^{2-}$$

Scheme 1 Suggested possible reaction pathway. Note that the heterogeneous electron transfer steps following the rate-determining step might be replaced by disproportionation reactions.

where n is total number of electrons transferred in the oxidation of Cr(III) to Cr(VI), D the diffusion coefficient ($cm^2\ s^{-1}$), C_0 the bulk concentration of the analyte (mol cm^{-3}), A the area of the electrode (cm^2) and V the potential sweep scan rate ($V\ s^{-1}$). Values for α_{an} and n', deduced from eqn. (2) were of 0.62 and 1 respectively. This produced an approximate value of the diffusion coefficient of $(2.3 \pm 0.2) \times 10^{-5}\ cm^2\ s^{-1}$, which was further refined to $(2.0 \pm 0.2) \times 10^{-5}\ cm^2\ s^{-1}$ as a result of the DIGISIM modeling[18] (see below).

3.3 DIGISIM modeling of the reaction for the Cr(III)/Cr(VI) couple

From eqn. (1) the value of E^0 at pH 13 was found to be −0.079 V *vs.* SHE (or −0.321 V *vs.* SCE) at 25 °C. Even though it is impossible to ascertain whether there are intermediate products in the oxidation process, some observations can be made: this is a multi-step reaction, and this involves an initial irreversible electron transfer which is rate-determining. Scheme 1 outlines a possible reaction pathway, where the first rate-determining electron transfer is followed by two electron transfer or disproportionation reactions.

Each of the three electron transfers involved in the oxidation of Cr(III) to Cr(VI) has an independent formal potential defined as E_1^0, E_2^0 and E_3^0. The average of these should be equal to the formal electrode potential of the reaction:

$$-FE^0_{Cr(III)/Cr(VI)} \times 3 = -FE_1^0 - FE_2^0 - FE_3^0$$
$$E^0_{Cr(III)/Cr(VI)} = \frac{(E_1^0 + E_2^0 + E_3^0)}{3} \qquad (4)$$

In order to simulate the experimental voltammograms E_2^0 and E_3^0 were set very negative of E_1^0 subject to the constraint of eqn. (4). For example, it was found that values of 0.00 V, −0.48 V and −0.48 V (all *vs.* SCE) for E_1^0, E_2^0 and E_3^0, respectively, produced voltammograms with a single oxidation peak of Cr(III) around the same position as that obtained experimentally. This applied for all scan rates studied if a heterogeneous rate constant value of 1.2×10^{-3} cm s^{-1} was assumed for the first electron transfer and those heterogeneous rate constants related to E_2^0 and E_3^0 were relatively fast (electrochemically reversible). However, it should be noted that none of these values necessarily or likely corresponds to the true values of the formal potentials nor can the value of 1.2×10^{-3} cm s^{-1} be attributed to the electrochemical rate constant since the process is electrochemically fully irreversible. Accordingly the values used in the DIGISIM modelling for the rate constants and the standard (formal) potential are not independent: only the transfer coefficient, α_{an}, can be inferred. Setting the value of the electron transfer coefficient for the first electron transfer to 0.7 was found to produce an excellent fit between the experimental and modelled waveshapes (Fig. 3A). The two other electron transfer reactions were set as fast reversible reactions.

Fig. 3B illustrates plots of modelled and experimentally obtained peak currents against square root of scan rate; the good agreement obtained confirms the suggested reaction pathway, whereby the first electron transfer is the rate-determining electrochemically irreversible reaction.

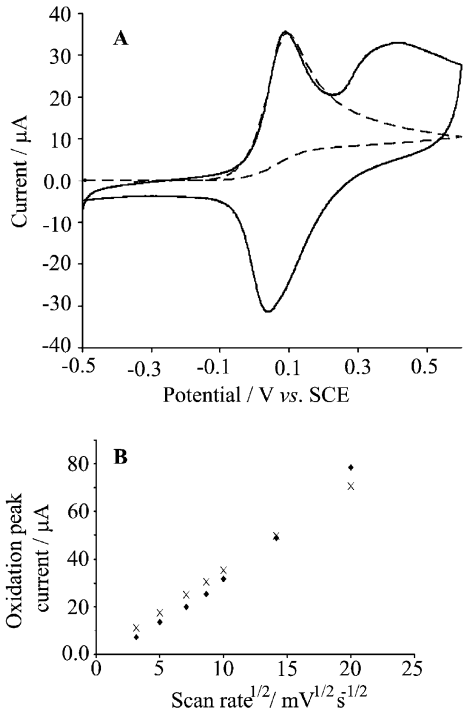

Fig. 3 A: comparison of modelled (dashed line) and experimentally obtained (solid line) cyclic voltammograms obtained for the oxidation of 500 μM Cr(III) (scan rate = 100 mV s^{-1}) at a gold electrode (A = 0.07 cm^2) in 0.1 M KOH. B: comparison of the corresponding plots of oxidation peak current against concentration of chromium(III) added based on experimentally obtained (◆) and modelled (×) data for a 0.1 M KOH solution.

3.4 Elucidation of the number of protons in the rate-determining step

The response of the gold electrode towards increasing additions of trivalent chromium in 1 M KOH was recorded next. The response of the gold electrode obtained in blank 1 M KOH (Fig. 4, dashed line) revealed a voltammetric profile similar to those shown in Fig. 1. However, the peaks attributed to the formation of an anodic "oxide" film and the film stripping processes were found to occur at more negative potentials: +0.30 V and +0.01 V for oxidation and reduction respectively. This can be explained by the release of H^+ during the formation of the gold film (Scheme 2e). Subsequently, the oxidation of trivalent chromium registered at −0.01 V (*vs.* SCE) shifted by *ca.* 88 mV towards negative values in comparison to the one recorded in 0.1 M KOH. This suggests hydroxide anion transfer is involved in the rate-determining step (Scheme 1, reaction 1). The increase in oxidation peak current measured at −0.01 V was found to be linear with concentration of trivalent chromium added to 1 M KOH in the range of 100 to 1000 μM

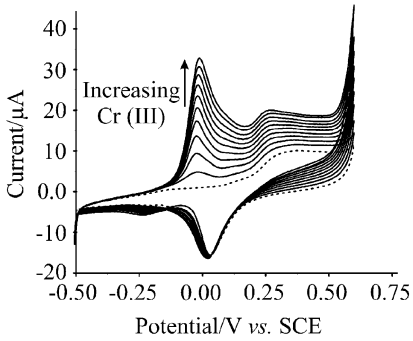

Fig. 4 Cyclic voltammograms (scan rate = 50 mV s^{-1}) detailing the response of increasing additions of aqueous Cr(III) (100–1000 μM) in 1 M KOH at an activated (ten cycles from −0.5 V to +0.6 V in 1 M KOH) gold electrode. Dashed line: response of the activated gold electrode recorder in 1 M KOH (scan rate = 50 mV s^{-1}).

(gradient = 3.4×10^{-2} A M^{-1}, $R^2 = 0.99$). As the magnitude of the peak current was similar in both pHs studied, eqn. (5)[19] can be applied to determine number of protons transferred in the RDS:

$$\frac{\partial E_p}{\partial \mathrm{pH}} = \frac{2.303mRT}{\alpha_{an} n' F} \qquad (5)$$

where m is the number of protons to be deduced, and α_{an} and n' are defined above and equal to 0.7 and 1 respectively. Substitution of the peak potential difference obtained at pH 13 and 14 provided a value for the number of the protons participating in the RDS equal to 1. This is consistent with the suggested reaction mechanism outlined in Scheme 1.

However the exact reaction mechanism remains to be evaluated further, as the process is complicated and likely involves oxygen containing species, which are probably chemisorbed on the electrode.[10] It is worth noting, that the increase in the oxidation current at +0.30 V (*vs.* SCE) observed with increasing additions of Cr(III) reflects the "tail" of the trivalent chromium oxidation wave analogous to that reported in Fig. 1.

3.5 Electrode "oxide" film growth

Scheme 2[20] summarizes reactions ascribed to the various potential regions, which occur at a bare gold electrode in alkaline conditions. It can be seen that in the potential range used in this paper three processes may occur: formation of adsorbed $Au(OH)^-$species as a result of the reaction of gold with the OH^-species in electrolyte (reaction c); formation of a monolayer of gold oxide (Au_2O_3), which develops into a multilayer at higher potential ($E > +0.39$) (reactions d and e); and oxygen evolution (reaction f). Moreover, it was found that the reversible adsorption of OH^- species observed below −0.04 V, becomes an irreversible process if higher potentials (0.5 V *vs.* SCE) are applied.[16]

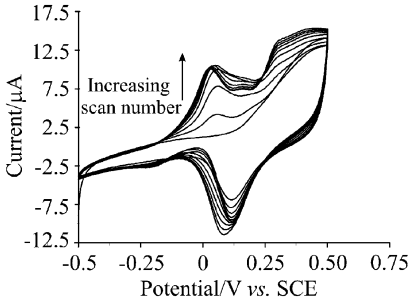

Fig. 5 Cyclic voltammograms (scan rate = 50 mV s^{-1}) detailing the oxidation of 500 μM Cr(III) during consecutive scans (1–10) at non-activated gold electrode in 0.1 M KOH.

Fig. 5 illustrates cyclic voltammograms obtained at a freshly polished gold electrode during ten consecutive scans in 0.1 M KOH solution containing 500 μM Cr(III). It can be seen that no significant oxidation process at +0.07 V was detected on the first scan; however a characteristic oxidation wave at +0.4 V and reduction wave at +0.07 V, attributed to multilayer formation and reduction of gold oxide (Au_2O_3) (Scheme 2),[20] was observed. On the second scan an oxidation wave emerged at the potential +0.07 V, analogous to that shown in Fig. 1; this continued to grow with a further five scans. This suggests that the Cr(III) oxidation process may involve OH^- species adsorbed on the electrode surface during the scan below −0.04 V as outlined in Scheme 2 (reaction c). In particular we note that at the potentials of interest Desilvestro and Weaver[16] suggested that the surface active species is $Au(OH)^-_{ads}$. At higher potentials, but more positive of those required for oxidation of Cr(III), the surface species $Au(OH)_{ads}$ is formed via the electron transfer: $Au + OH^- - e^- \rightleftharpoons Au(OH)_{ads}$ Accordingly we might suggest $Au(OH)^-_{ads}$ may be an intermediate in the oxidation of Cr(III). However this does not explain why potential excursions to or beyond +0.6 V (*vs.* SCE) are required to see the Cr(III) oxidation. In a previous paper concerned with anodic stripping voltammetry[21] we have demonstrated that the removal of metallic deposits from an electrode surface by means of an anodic potential scan is often incomplete and that significant deposits can remain even after the electrochemical stripping peak is seemingly "finished". We therefore speculate that a similar phenomenon may occur in the present case and that after cycling into the "Au_2O_3 region" some metal oxide is present even at potentials cathodic of the stripping peak at +0.07 V and this may likely be a key intermediate in the Cr(III) oxidation.

To examine if the process is surface based, the electrode was cycled in the solution containing Cr(III) species, then rinsed and dipped in the blank 0.1 M KOH solution. Three repetitive scans were then performed. The resulting voltammetric profiles revealed the appearance of the Cr(III) oxidation peak at +0.07 V, which diminished completely with further scans.

-1.42 V <E< -0.84 V (vs. SCE):	$H_2O + e^- \rightarrow H_{ads} + OH^-$	θ_H=1	(a)
-0.84 V <E<-0.44 V (vs. SCE):	$H_2O + e^- \rightarrow H_{ads} + OH^-$	θ_H<1	(b)
-0.44 V <E< -0.04 V (vs. SCE):	$Au + OH^- \rightarrow Au(OH)^-_{ads}$	$\theta_{AuOH} \leq 1$	(c)
-0.04 V<E< +0.39 V (vs. SCE):	$2Au + 3H_2O \rightarrow Au_2O_3 + 6H^+ + 6e^-$	$\theta_{Au2O3} \leq 1$	(d)
E> +0.39 V (vs. SCE):	$2Au + 3H_2O \rightarrow Au_2O_3 + 6H^+ + 6e^-$	multilayer	(e)
E> +0.39 V (vs. SCE):	$2H_2O \rightarrow O_2 + 4H^+ + 4e^-$		(f)

Scheme 2 Reactions of a bare gold surface in 1.0 M KOH adapted from ref. 19. θ_X represents the coverage of species X.

Next a set of cyclic voltammograms with varying surface conditioning parameters were recorded. It was found that if the response was recorded in a 0.1 M KOH solution containing 500 μM Cr(III) in the region between −0.5 V and +0.25 V, in order to avoid the "oxide region" starting at +0.3 V, the resulting voltammograms (not shown) revealed no oxidation process for Cr(III) in the potential range studied.

However, as described above the oxidation peak for Cr(III) at +0.07 V emerged during the second scan between the potential limits of −0.5 V and +0.6 V in a solution of 500 μM Cr(III) in 0.1 M KOH. This was found to disappear within three scans if cycling was subsequently restricted to between −0.5 V and +0.25 V only. However, if pre-conditioning of the electrode for 10 seconds at +0.6 V was applied prior to commencing each scan in the same solution and in the same scan range of −0.5 V to +0.25 V, the characteristic oxidation process at +0.07 V was again observed. The magnitude of the peak current measured at +0.07 V was found to increase linearly with further additions of Cr(III) in the range of 100–1000 μM (gradient = 1.87×10^{-2} A M^{-1}, $R^2 = 0.99$). However, it can be seen that the magnitude was lower than those outlined in Fig. 1; the data shown in the figure corresponds to the conditions when the oxidation is diffusion controlled. With less than optimal electrode pre-treatment the surface may not be fully active to the oxidation of Cr(III).

This phenomenon was investigated further: data obtained after various pre-treatment conditions are summarized in Fig. 6. It can be seen that the most active surface with respect to the oxidation of trivalent chromium was achieved using ten consecutive cycles between −0.5 V and +0.6 V in 0.1 M KOH. It is worth noting that based on the data outlined in Fig. 5, the number of scans might be limited to five. The activity was found to decrease if the scan range was extended to +0.8 V, which might be due to the further oxidation of either $Au(OH)_{ads}$[22] or Au_2O_3 species.[15] Examination of Fig. 6 shows that holding at a positive potential (+0.6 V or +0.8 V) for 220 s (the time required for five scans between −0.5 V and +0.6 V at 50 mV s^{-1}) caused a decrease in activity of the oxidation process, indicating the importance of the cathodic scan. Electrochemical cycling may create more separate sites of incomplete stripped Au_2O_3 with adsorbed OH^- species, which then take part in trivalent chromium oxidation via the mechanism suggested in Scheme 1. In order to explore this hypothesis AFM studies were carried out next.

3.6 AFM examination of electrode morphology

In-situ AFM was used to attempt to correlate large scale morphological changes occurring on the gold surface with the pre-treatments described in the previous section. Four sets of pre-treatment conditions in 0.1 M KOH were considered: cycling between the limits −0.6 V and +0.6 V, −0.8 V and +0.8 V, a potential step to +0.6 V, and a potential step to +0.8 V.

In the cases in which potential cycling was applied, the following procedure was followed: the AFM scanner was engaged with the cell set to the open circuit potential, and several scans performed at a scan rate of 4 Hz to allow the scanner position to stabilize. After collecting an initial image of the freshly polished surface, the AFM tip velocity was set to zero. A cyclic potential was applied from 0 V to the positive potential limit, then back to 0 V at 50 mV s^{-1}, after which the cell was switched off. Another image was then collected at 4 Hz, the tip stopped again, and a similar cycle applied between 0 V and the negative potential limit. This process was repeated until 10 complete cycles had been performed. A similar procedure was used in the cases where a potential step was applied, except that a constant potential was applied for a given time between the collection of each AFM image.

It was found that both cycling between −0.6 V and +0.6 V and applying a potential of +0.6 V for up to 220 seconds resulted in no observable large scale (1 μm) change in the gold surface morphology. This is consistent with previous AFM experiments performed in acid,[23] which showed full oxidation of the gold surface generated only 1–2 monolayers of oxide. Analysis of the charge transferred during the scan from 0 V to +0.6 V agrees with this: although the manually polished surface has an ill-defined surface roughness, making precise coverage calculations difficult, the charge transferred is approximately consistent with 1–3 non-uniform layers of oxide. We would not expect a surface change this small to be visible on the relatively large scale at which the AFM was performed.

The freshly polished gold surface, covered in a distinctive network of polishing scratches, is shown in Fig. 7A, having a root mean square (RMS) roughness (calculated by computing the square root of the sum of all powers in the 2D power spectral density spectrum) of 2.53 ± 0.11 nm. The same area after applying a potential of +0.8 V for 30 s is shown in Fig. 7B. Although the scanner has drifted by approximately 200 nm, the same features are visible. The surface appears smoother, with some coalescence of grains occurring: the RMS roughness is now 1.26 ± 0.03 nm. Further oxidation up to 220 seconds resulted in no further changes to the surface morphology. The changes were found to be reversible: on applying −0.8 V, the surface reverted almost immediately to its initial appearance.

Next potential cycles from −0.8 V and +0.8 V were applied; the clean surface is shown in Fig. 8A. The R_a values (defined as the arithmetic mean of the absolute values of the surface height deviations measured from the mean plane) for the clean surface and each successive scan are shown in Fig. 9. It appears that both positive and negative cycles generally decrease the roughness of the surface, with some exceptions, notably the fifth, sixth, and ninth positive cyclic voltammograms. The images collected after these are shown in Figs. 8B, C and D, respectively. The changes responsible for the increases in R_a are highlighted: it appears that applying the positive cycle generates the larger particles of oxide observed in Fig. 8B, C and D independently of the surface smoothing effect.

This AFM analysis supports the notion of gold oxide involvement in the Cr(III) oxidation process. As Fig. 9 shows, the reduction cycles (from 0 V to −0.8 V to 0 V) cause relatively small decreases in roughness; the oxide features responsible for the large R_a increases are largely unaffected. This may be an example of the recently reported phenomenon of incomplete stripping,[21] and suggests that the partly reduced oxide is important to the Cr(III) oxidation. Although no similar large oxide features appear when cycling to +0.6 V a similar process is probably in operation; it is likely the oxide particles

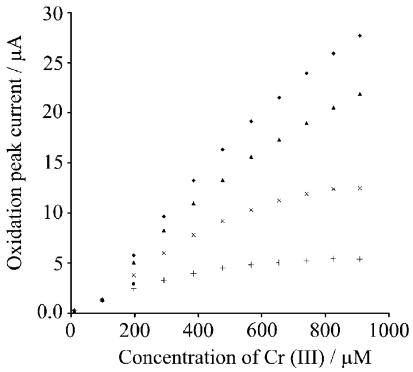

Fig. 6 Corresponding plots of oxidation peak current against concentration of Cr(III) recorded after different electrode pre-treatment conditions: ten cyclic voltammetry scans between −0.5 V and +0.6 V (◆), ten cyclic voltammetry scans between −0.5 V and +0.8 V(▲), holding for 220 s at +0.8 V (×) and holding for 220 s at +0.6 V (+). Pre-treatment in all cases was carried out in 0.1 M KOH.

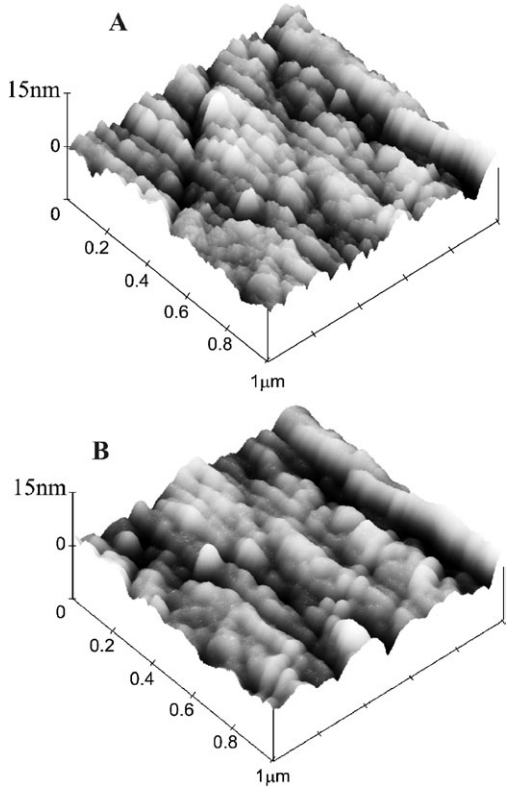

Fig. 7 *In-situ* AFM images of (A) manually polished gold and (B) the same area after oxidation at +0.8 V *vs.* SCE for 30 seconds in a 0.1M KOH solution.

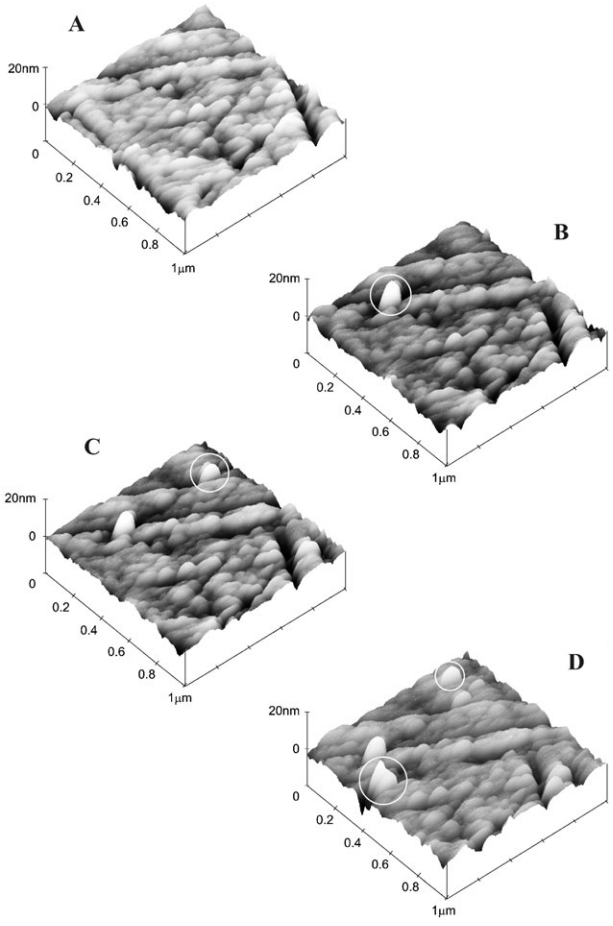

Fig. 8 *In-situ* AFM images of (A) manually polished gold, (B–D) the same area after the fifth, sixth and ninth oxidation CV from 0 V to +0.8 V at 50 mV s^{-1} (see text for the details). The circles highlight newly appeared large grains.

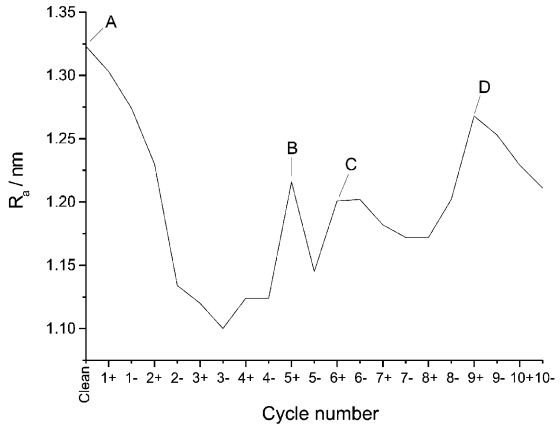

Fig. 9 A plot of surface roughness (R_a, see text) *vs.* cycle number for the dataset illustrated in Fig. 7. 'n+' indicates a scan was performed from 0 V to +0.8 V to 0 V at 50 mV s^{-1} before the R_a value was measured. 'n−' indicates a scan was performed from 0 V to −0.8 V to 0 V at 50 mV s^{-1} before the R_a value was measured. A–D refers to the points at which the scans A–D are shown in Fig. 8.

generated are much smaller and therefore undetectable at the scan ranges employed.

4. Conclusions

The oxidation of trivalent chromium (500 μM) was examined at various electrode substrates over a wide pH range. A distinctive voltammetric profile was recorded only in an alkaline media (pH greater than 12) at a polycrystalline gold electrode. It was shown that the reaction proceeds via a multi-step mechanism, whereby the first step is rate-determining and involves electrochemically irreversible electron transfer as well as the transfer of a OH^- ion. The two or more following steps are fast and might either proceed via further electroxidation of the newly formed Cr(IV) species or via disproportionation pathways. The observed data has been successfully modelled using DIGISIM with a transfer coefficient of 0.7 deduced for the first rate-determining step. Furthermore it was found that activity of the electrode towards oxidation of Cr(III) species depends on the pre-treatment of the gold electrode with potential cycling to anodic limits essential for good electrocatalysis towards Cr(III) oxidation. AFM and other measurements suggest that this comes from incomplete stripping of the Au_2O_3 formed in this way. The role of the Au_2O_3 is not fully clear; however we speculate that the nature of the adsorbed species, especially OH^-, may change accordingly to the presence or absence of the oxide.

Acknowledgements

MEH thanks EPSRC for his project studentship. ON expresses her gratitude to the Analytical Division of the RSC for the award of a studentship.

References

1 M. Cespon-Romero, M. C. Yebra-Biurrun and M. P. Bermejo-Barrera, *Anal. Chim. Acta*, 1996, **327**, 37.
2 World Health Organization, 2004, http://www.who.int/docstore/water_sanitation_health/.
3 B. R. G. Danielsson, E. Hassoun and L. Dencker, *Arch. Toxicol.*, 1982, **51**, 233.
4 S. De Flora, M. Banasco, D. Serra and P. Zanacchi, *Mutat. Res.*, 1990, **238**, 99.
5 W. Qi, R. J. Reiter, D-X. Tan, J. J. Garcia, L. C. Manchester, M. Karbownik and J. R. Calvo, *Environ. Health Perspect.*, 2000, **108**, 399.

6 D. Golub and Y. Oren, *J. Appl. Electrochem.*, 1989, **19**, 311.
7 R. J. Kieber, J. D. Willey and S. D. Zvalaren, *Environ. Sci. Technol.*, 2002, **36**, 5321.
8 G. H. Kelsall, C. I. House and F. P. Gudyanga, *J. Electroanal. Chem.*, 1988, **244**, 179.
9 P. Zanello and G. Raspi, *Anal. Chim. Acta*, 1977, **88**, 237.
10 I. Danilov and A. B. Velichenko, *Electrochim. Acta*, 1993, **38**, 437.
11 R. I. Stefan, S. G. Bairu and J. F. Van Staden, *Anal. Bioanal. Chem.*, 2003, **376**, 844.
12 E. Deltombe, N. de Zoubov, M. Pourbaix, in *Atlas of Electrochemical Equilibria in Aqueous Solutions*, ed. M. Pourbaix, Pergamon Press, New York, 1966, pp. 256–271.
13 C. M. Welch, O. Nekrassova and R. G. Compton, *Talanta*, 2004, in press.
14 B. Beden, I. Cetin, A. Kahayaoglu, D. Takky and C. Lamy, *J. Catal.*, 1987, **104**, 37.
15 L. D. Burke, D. T. Buckley and A. J. Morrissey, *Analyst*, 1994, **119**, 841.
16 J. Desilvestro and M. J. Weaver, *J. Electroanal. Chem.*, 1986, **209**, 377.
17 D. W. Kirk, F. R. Foulkes and W. F. Graydon, *J. Electrochem. Soc.*, 1980, **127**, 1069.
18 M. Rudolph, D. P. Reddy and S. W. Feldberg, *Anal. Chem.*, 1994, **66**, 589.
19 P. Zuman, *The Elucidation of Organic Electrode Processes*, Academic Press, New York, London, 1969.
20 R. C. Newman and G. T. Burstein, *J. Electroanal. Chem.*, 1981, **129**, 343.
21 M. E. Hyde, C. E. Banks and R. G. Compton, *Electroanalysis*, 2004, **16**, 345.
22 R. Cordova, O. M. E. Martins and A. J. Arvia, *Electrochim. Acta*, 1980, **25**, 453.
23 S. Manne, J. Massie, V. B. Elings, P. K. Hansma and A. A. Gewirth, *J. Vac. Sci. Technol. B*, 1992, **9**, 950.